Reversible electrochemical modulation of fluorescence and selective sensing of ascorbic acid using a DCIP-CA-CdTe QD system

Cong Kong,[a] Da-Wei Li,[a] Yang Li,[a] Raheleh Partovi-Nia,[a] Tony D. James,[c] Yi-Tao Long[a] and He Tian*[b]*

[a] Shanghai Key Laboratory of Functional Materials Chemistry & Department of Chemistry, East China University of Science and Technology

[b] Key Laboratory for Advanced Materials and Institute of Fine Chemicals, East China University of Science and Technology

[c] Department of Chemistry, University of Bath, Bath, BA2 7AY, UK

Preparation of fresh sodium hydrogen telluride (NaHTe) solution

Fresh sodium hydrogen telluride (NaHTe) solution was prepared in accordance with previous references.[1] Briefly, NaBH4 (0.1284 g) was added to a small flask. Deionized water (10 mL) and tellurium (0.076 g) powder were then added in the flask, and the mixture was stirred gently at room temperature. During the reaction, high purity nitrogen was injected into the flask to eliminate the oxygen and protect the fresh NaHTe against oxidation. About 4 hours later, the black tellurium powder disappeared and the resulting NaHTe in clear purple supernatant was generated to prepare the CdTe QDs.

Preparation of CdTe QDs

Positively charged CA-CdTe QDs (with cysteamine as a stabilizing agent) were synthesized in aqueous solution by previously reported procedures with minor revisions.[2] Ultrapure water (100 ml) and CdCl2•2.5H2O (300 mg) were added to a 250 ml flask with stirring. Cysteamine (1.5g) was added into the mixture. The pH of the reaction solution was adjusted to 5.0 with concentrated NaOH (1 M). The above mentioned fresh sodium hydrogen telluride (NaHTe) solution was added into the reaction flask with continuous and vigorous stirring under an N2 atmosphere. The feed molar ratio of Cd^{2+}/cysteamine/NaHTe was 1:10:0.46. The reaction solution was kept stirring for 8 hours at 90 ℃. The initial brown solution turned reddish clear. High fluorescence was observed after the enough reaction time, suggesting the formation of CdTe nanocrystals. The cysteamine capped QDs was cooled down to room temperature, precipitated by the addition of acetone, separated by centrifugation, washed with acetone, and dried with high purity nitrogen.

Furthermore, negatively charged CdTe quantum dots (MPA-CdTe QDs) with the MPA as the stabilizing agent were synthesized in aqueous solution by similar procedures,[3] except that the feed molar ratio of Cd^{2+}/MPA/NaHTe was 1:1.3:0.46. Before addition of NaHTe solution, pH of MPA and $CdCl_2$ mixture was adjusted to 11.

UV-Vis absorption and fluorescence spectra

The UV-Vis absorption spectra were obtained on an Ocean Optics USB2000+ (190~1700 nm), UV-Vis Miniature Fiber Optic Spectrometer using a high-performance 2048-element linear CCD-array detector and DT-mini-2 light source. Fluorescence measurements were carried out on an Ocean Optics USB400 fiber- optic spectrometer (400 ~ 1000nm), by excitation at 365 nm with an light source (LE-SP-LS-XE 500, Shenzhen Leo-photoelectric Co., Ltd. China). In situ monitoring of the absorption and fluorescence profile of DCIP-CA-CdTe QD under electrochemical

modulation was performed in the same setup except that an indium tin oxide working electrode (thickness, 1.2mm), a Ag/AgCl reference electrode and a Pt wire counter electrode were inserted into the cuvette (Light path of the cuvette is only 1.5mm, as ITO working electrode was inserted in the cuvette, a thin layer of 0.3mm solution left in the process of absorption and fluorescence modulation) to carry out electrochemical experiments at room temperature using a CHI 1232A electrochemical workstation (Shanghai Chenhua Co. Ltd., China). As a result, the evolution of the absorption and fluorescence spectra of the solution could be recorded in real time. Transmission electron microscopy (TEM) images were captured using a JEM-2100 (JEOL, Japan).

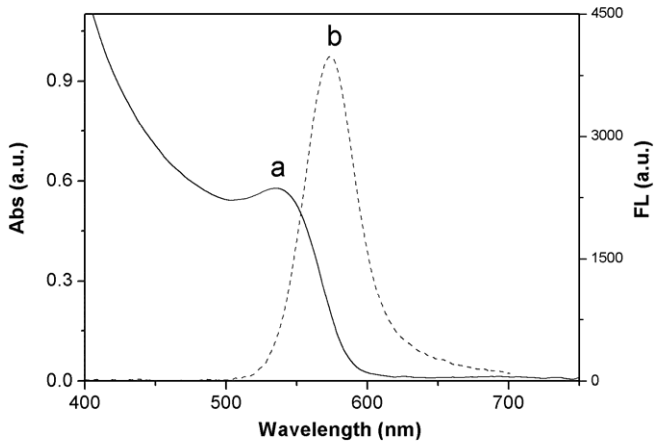

Figure S1. Absorption (a) and fluorescence (b) spectra of CA-CdTe QDs (3 μM), excitation wavelength: 365 nm.

Spectroscopic properties of CA-CdTe QDs are shown in **Figure S1**. The UV-Vis absorption spectrum of the CA-CdTe QDs shows a sharp peak centered around 540 nm (**Figure. S1a**), indicating that the particle size distribution was relatively narrow. **Figure S1b** depicts the fluorescence spectra of CA-CdTe QDs with a pronounced peak at 574 nm, which has a half peak width of approximately 42 nm. The fluorescence spectrum of the CA-CdTe QDs displayed clear band-edge recombination without any trap-state related emission. The shape and diameter of the CA-CdTe QDs were characterized by TEM. The average size of the CA-CdTe nanoparticle was approximately 4 nm, as shown in **Figure S2**, where QDs are clearly monodispersed, which is in consistent with the result calculated by the excitonic absorption peak.

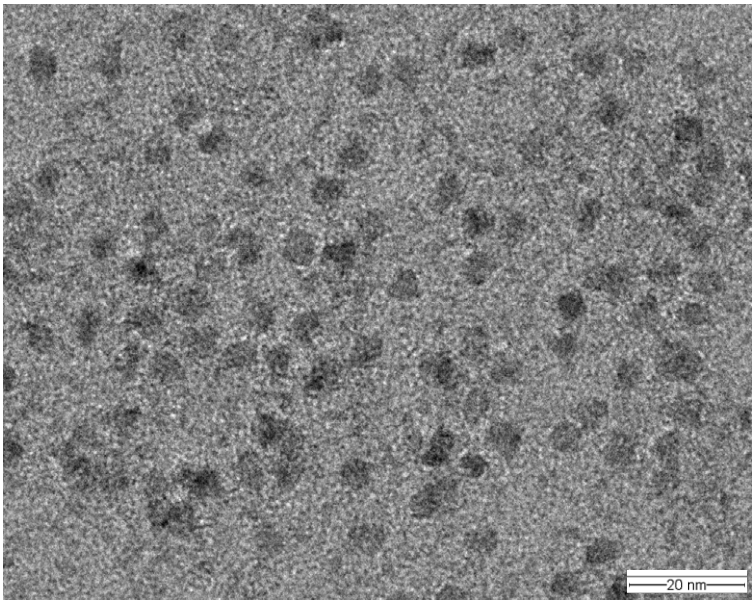

Figure S2. TEM image of CA-CdTe QDs.

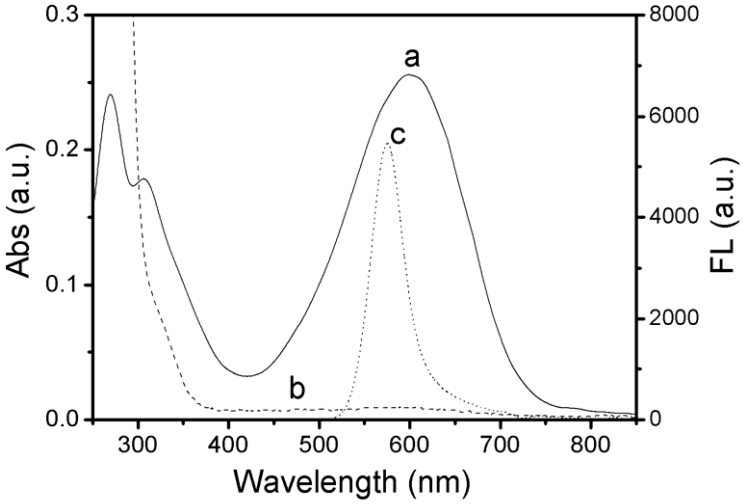

Figure S3. Absorption spectra of DCIP in the absence (a) and presence (b) of AA. (c) Fluorescent emission spectrum of CA-CdTe QDs.

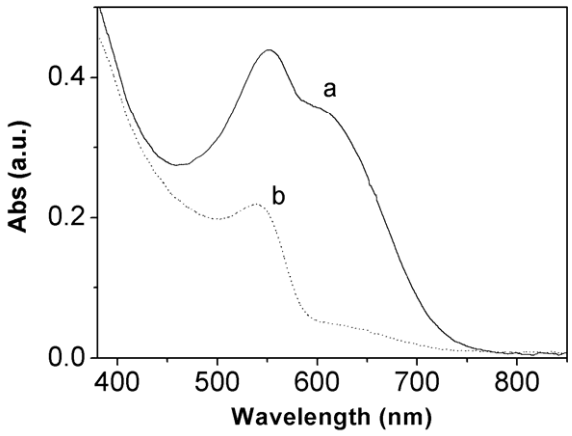

Figure S4. Absorption profile of CA-CdTe QDs (a) in the presence of DCIP (15 μM) and (b) upon further addition of excess AA.

UV-vis absorption spectroscopy is a simple method for examining changes in a compound and the interaction between CA-CdTe QDs and DCIP. After addition of DCIP to the aqueous CA-CdTe QD solution, the spectrum of the deep blue solution contained another pronounced peak at 600 nm (**Figure S4a**) compared with the initial sharp peak at 540 nm. The capping molecules (cysteamine) were positively charged on the surface of the CA-CdTe QDs, while DCIP was negatively charged in a solution of the same pH. As these molecules were oppositely charged, it is reasonable to expect that the small DCIP molecules would be absorbed onto the CA-CdTe QDs through attractive electrostatic interactions. After the introduction of AA into the solution, which was degassed to eliminate oxygen, the intensity of the 600-nm absorption peak decreased gradually within 3 minutes (**Figure S4b**) and finally disappeared, making the solution nearly transparent with a slight red color. The apparent color change can be attributed to the reduction of DCIP by AA in solution.[4, 5]

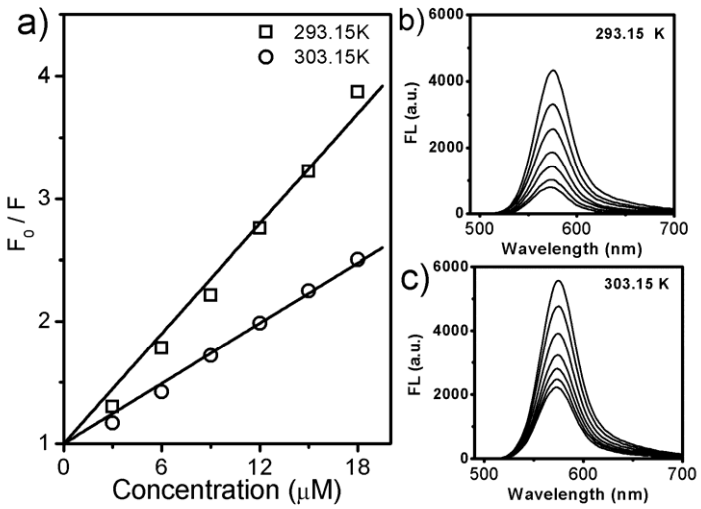

Figure S5. (a) Stern-Volmer plot of the fluorescence quenching of CdTe QDs by DCIP at different temperatures. (b) Fluorescence quenching profile of DCIP on the CA-CdTe QDs at 293.15 K, corresponding to the squares in (a). (c) Fluorescence quenching profile of DCIP on the CA-CdTe QDs at 303.15 K, corresponding to the circles in (a).

In order to confirm the quenching mechanism, we analyzed the fluorescence quenching data with well known Stern–Volmer plot. The quenching effect is generally classified as either a dynamic or static quenching mechanisms. Dynamic quenching refers to a process where the fluorophore (CA-CdTe QDs) and the quencher (DCIP) come into contact during the transient existence of the excited state while static quenching refers to the formation of fluorophore–quencher complex. The Stern–Volmer equation in analysis of fluorescence quenching is as follows:

$$\frac{F_0}{F} = 1 + \kappa_q \tau_0 [Q] = 1 + \kappa_{sv} [Q]$$

where F_0 and F are the fluorescence intensities before and after the addition of the quencher (DCIP), κ_q, κ_{sv}, τ_0, and [Q] are the quenching rate constant of the molecule, the Stern–Volmer quenching constant, the average lifetime of the fluorophore without quencher and the concentration of the quencher, respectively. The Stern–Volmer plots of F_0/F versus [Q] at two different temperatures (293.15 K and 303.15 K) are shown in **Figure S5**. The results show that the Stern–Volmer quenching constant κ_{sv} is inversely correlated with increasing temperature, demonstrating that the quenching effect of DCIP on the CA-CdTe QDs was initiated by complex formation rather than dynamic interaction.[6-8]

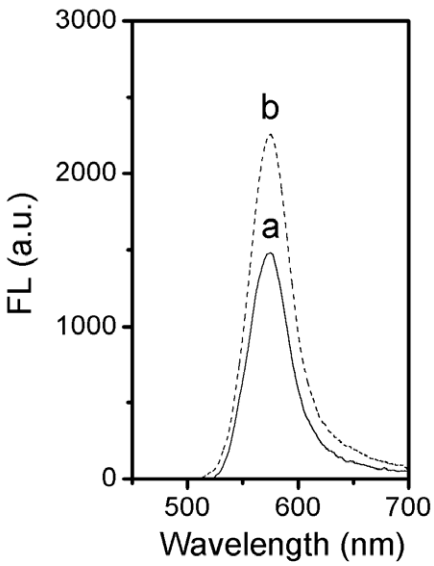

Figure S6. Fluorescence profile of DCIP-CA-CdTe QDs (20 μM DCIP, 2 μM CdTe QDs) in the (a) absence (solid line) and (b) presence (dashed line) of KCl (10 mM).

When an electrolyte (KCl) was added to the complex solution, the fluorescence increased due to the desorption of DCIP from the CA-CdTe QDs, as shown in **Figure S6**. These results further confirm the electrostatic charge interaction between the negatively charged DCIP molecules and positively charged CA-CdTe QDs, which accounts for the efficient fluorescence quenching.

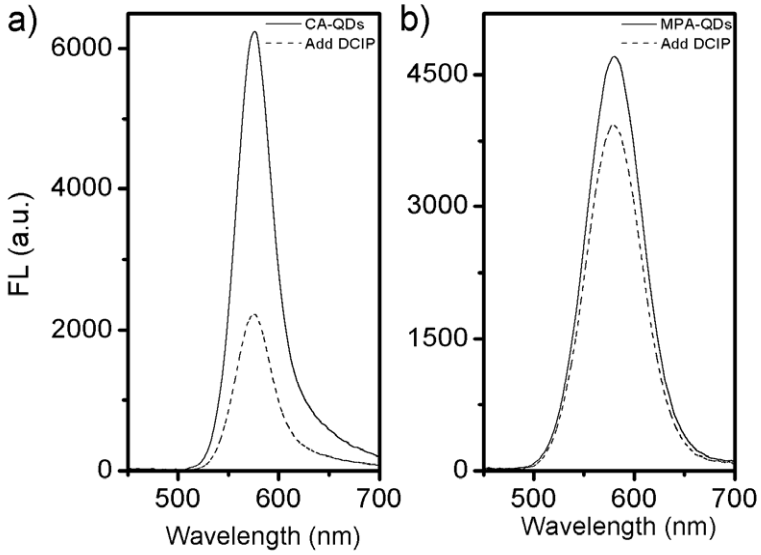

Figure S7. Fluorescence quenching profile of CdTe QDs by DCIP: (a) Fluorescence of positively charged QDs (2 μM CA-CdTe QDs, solid line) and further addition of DCIP (20 μM, dashed line). (b) Negatively charged QDs (2 μM MPA-CdTe QDs, solid line) and further addition of DCIP (20 μM, dashed line).

The FRET quenching process occurred on the surface of the CA-CdTe QDs based on the close proximity of energy donor and acceptor. Hence, the electrostatic interactions between CA-CdTe QDs and DCIP would affect on the contact of them, and further determine the quenching process. To demonstrate the charge effect, we investigated the quenching efficiency of DCIP on CdTe QDs with different surface charge properties. Fluorescence quenching profiles were obtained when DCIP was added to equivalent concentrations of the positively and negatively charged MPA-CdTe QDs, as shown in **Figure S6**. There was a clear difference in DCIP quenching efficiency for the oppositely charged solutions with a high quenching efficiency (approximately 74%) for the positively charged solution (**Figure S6a**) compared with that of the negative solution (approximately 17%) (**Figure S6b**). This result further confirmed that the quenching effect of DCIP on the CA-CdTe QDs arises from complex formation through electrostatic interactions. The more efficient fluorescence quenching was obtained using the positively charged CA-CdTe QDs, rather than the negatively charged CA-CdTe QDs.

Effect of acidity on fluorescence

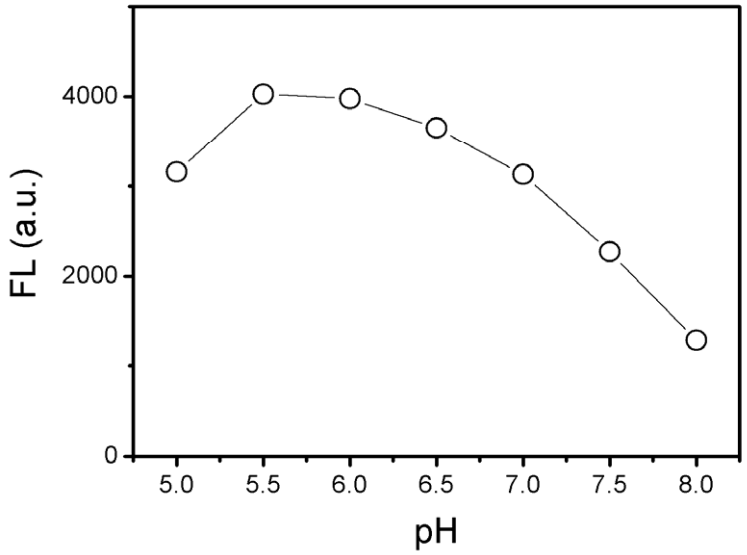

Figure S8. Fluorescence recovery profile of DCIP-CA-CdTe QDs (DCIP 20 μM, CA-CdTe QDs, 3 μM) by AA (40 μM) at different pH.

The influence of pH on the fluorescence recovery of the DCIP-CA-CdTe QD system was investigated. CA-CdTe QDs were more stable and exhibited better optical properties in acidic and weakly basic solutions than in basic solutions (**Figure S8**) because the fluorescence intensity was significantly influenced by the charge state of the surface amide groups. After addition of AA to the prequenched system, fluorescence recovery reached a maximum and remained stable over a pH range of 5.0–7.6. Moreover, the reducing ability of AA is pH dependent, which could affect the redox state of DCIP on the surface of the CA-CdTe QDs and further influence the fluorescence intensity of the solution. Based on these results, a pH of 6.0 was selected to ensure a highly selective and sensitive response to AA.

[1] Y.-C. Kuo, Q. Wang, C. Ruengruglikit, H. Yu, Q. Huang, *J. Phys. Chem. C* **2008**, *112*, 4818-4824.

[2] W.-h. Yang, W.-w. Li, H.-j. Dou, K. Sun, *Mater. Lett.* **2008**, *62*, 2564-2566.

[3] C. Schulz-Drost, V. Sgobba, D. M. Guldi, *J. Phys. Chem. B* **2008**, *112*, 14482-14491.

[4] S. Hartwell, W. Kochasit, S. Kerdphon, J. Jakmunee, S. Lapanantnoppakhun, T. Sanguansermsri, K. Grudpan, *Microchimica Acta* **2009**, *167*, 201-209.

[5] A. M. Sgaravatti, B. A. Vargas, R. Zandona Bernardo, K. B. Deckmann, F. J. Rockenbach, T. B. Moraes, J. M. Monserrat, M. B. Sgarbi, C. D. Pederzolli, A. T. S. Wyse, C. M. D. Wannmacher, M. Wajner, C. S. Dutra-Filho, *Int. J. Dev. Neurosci.* **2008**, *26*, 551-559.

[6] V. V. Breus, C. D. Heyes, G. U. Nienhaus, *J. Phys. Chem. C* **2007**, *111*, 18589-18594.

[7] A. M. Munro, I. Jen-La Plante, M. S. Ng, D. S. Ginger, *J. Phys. Chem. C* **2007**, *111*, 6220-6227.

[8] E. Mohamed Ali, Y. Zheng, H.-h. Yu, J. Y. Ying, *Anal. Chem.* **2007**, *79*, 9452-9458.